

Generation of femtosecond X-ray pulse pairs

X-ray free-electron lasers (XFELs), such as SACLA, provide intense, ultrashort X-ray pulses that can probe matter at the atomic length scale and femtosecond time scale. The standard operation of XFELs uses self-amplified spontaneous emission (SASE) pulses that have a $\sim 0.5\%$ relative spectral bandwidth and consist of many random narrow spectral and temporal spikes. Secondary monochromators and new accelerator schemes, such as self-seeding, can provide single-color XFEL pulses with increased temporal coherence, yet, even such pulses limit the applications of XFELs to nonlinear coherent imaging and spectroscopy techniques that, in the optical domain, have revolutionized our understanding of the structures and dynamics of molecules and materials. Extending coherent nonlinear spectroscopies and imaging to the X-ray domain would provide direct insight into the coupled motions of electrons and nuclei, with resolution on the electronic length and time scale and elemental sensitivity. Several approaches have been proposed, but its experimental realization proves very difficult. One big challenge is the generation of intense, coherent, femtosecond X-ray pulses with fixed relative phases. Several groups are currently pursuing the creation and detection of coherent femtosecond X-ray pulse pairs. The work described here focuses on our recently published observation of generating intense phase-stable femtosecond hard X-ray pulse pairs [1].

Our approach for generating such X-ray pulse pairs is based on amplified spontaneous emission (ASE) and seeded stimulated emission (SSE). Both phenomena require intense XFEL pulses and have been observed and explored for various applications at X-ray energies ranging from 850 eV to 8 keV [2–4]. Our experiments were performed at the nanofocus instrument EH5 at SACLA BL3 XFEL providing highly focused SASE pump and seed pulses. Spectral analysis of the emission signal was performed using a flat Si (220) analyzer crystal dispersing the emission signal onto a two-dimensional CCD. We focus on the 5.9 keV (2.1 Å) Mn $K\alpha_1$ emission line, where we employ an intense XFEL pump pulse at 6.6 keV (above the Mn K -edge) to create many simultaneously excited $1s$ core holes. Stimulated X-ray emission can occur either in the form of ASE, where a randomly emitted X-ray fluorescence photon acts as the seed, or via SSE, where an external second-color XFEL pulse provides the seed. Figure 1 shows the level and state diagrams of stimulated $K\alpha$ X-ray emission (a), the concept of ASE and SSE (b), and the main

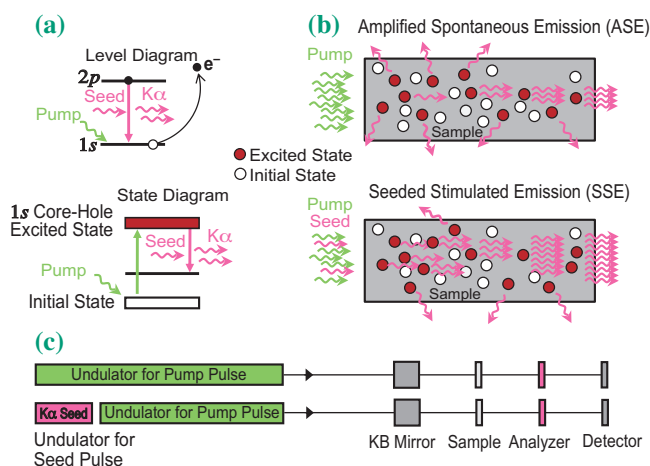


Fig. 1. (a) Level and state diagrams for stimulated $K\alpha$ X-ray fluorescence (red) following $1s$ core hole ionization by an incident photon (green) and seeding by either a spontaneously emitted fluorescence photon (ASE) or an external seed photon (SSE). (b) Concepts of the two types of stimulated X-ray emission. The pump pulse (green) creates $1s$ core-hole excited states (red). In ASE, a spontaneously emitted $K\alpha$ photon seeds the emission of a second $K\alpha$ photon along the direction of $1s$ core hole-excited states and so on, leading to amplification. In SSE, external seed pulse photons (magenta) stimulate the emission of $K\alpha$ photons from $1s$ core hole excited states along the seeding direction. (c) Schematics of the basic components for ASE and SSE experiments showing the undulators for pump and seed pulse generation, the KB focusing mirrors, the sample, the Bragg crystal analyzer, and the 2D detector.

experimental components (c).

When studying ASE and SSE signals from various Mn compounds at SACLA, we discovered that in some instances the observed spectra show strong interference fringes. Such fringes cannot be caused by any sample-related features in the X-ray emission. After ruling out several possible causes for these fringes, we found the cause: When a SASE XFEL pump pulses has two strong temporal spikes (in addition to many weak ones), each of these strong spikes has enough intensity to generate a very short (1 fs or less) highly directional ASE/SSE signal. The result is an X-ray pulse pair with temporal spacings of ~ 2 – 5 fs manifested by spectral interference fringes. The fringes constitute the time-frequency X-ray analogue of Young’s double-slit interference allowing for frequency-domain X-ray measurements with attosecond time resolution. The sequence of events for the generation of X-ray pulse pairs and interference fringes is illustrated in Fig. 2.

The relation between the spectral fringe spacings ΔE and temporal pulse spacings Δt is obtained through Fourier analysis via the Planck constant $\Delta t \Delta E = h = 4.136 \text{ fs} \cdot \text{eV}$. Single-shot spectra exhibiting values for ΔE (0.9–2.5 eV) and corresponding values for Δt (1.7–4.6 fs) are shown in Fig. 3. We used the 1-dimensional (1D) semi-classical Maxwell-Bloch theory [5] to simulate the spectra to establish the link between the temporal structure of the SASE pump pulses and the observed fringes.

The fact that stimulated emission is highly nonlinear can explain why in the weaker spikes of the SASE spectrum might not lower the observed contrast of the interference fringes: A temporal spike only generates stimulated emission once it reaches the threshold required for sufficient population inversion. This also explains why fringes are generally rare and their probability depends on the SASE temporal profiles resulting from the electron-bunch compression mode in the linear accelerator.

To conclude, we have experimental evidence that stimulated X-ray emission generated by an XFEL SASE pulse can result in phase-stable fs X-ray pulse pairs. The resulting spectral fringe pattern contains the information about the X-ray pulse pairs, including their temporal spacing, coherence, and relative phase.

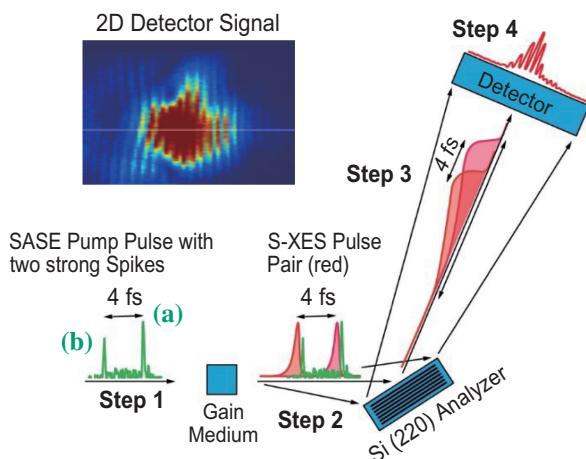


Fig. 2. XFEL SASE pump pulse with two strong temporal spikes (a), (b), impinges on the sample (Step 1), each creating a short superfluorescence burst. The two pulses leave the sample with a slight delay with respect to their respective SASE spikes given by the lifetime of the excited state (Step 2). The two pulses do not overlap temporally until they impinge on the analyzer crystal, where they are spectrally dispersed and temporally stretched to $\sim 22 \text{ fs}$ ($\sim 8 \text{ fs}$ FWHM) corresponding to the $\sim 0.24 \text{ eV}$ FWHM Si (220) resolution (Step 3). The two signals then create the frequency interference with the fringe spacings that are inversely proportional to their time delays (Step 4). Inset shows the measured 2D detector signal from a single pulse pair. The white line shows the cut along the dispersive direction resulting in the spectrum shown in Step 4. For more details see [1].

The spectral fringe separation directly encodes the time delay of these pulses, which can be determined with ~ 20 attosecond precision for measuring delays of $\sim 4 \text{ fs}$. A future, more robust method for obtaining phase-stable pairs of fs X-ray pulses by stimulated X-ray emission might pave the way to realizing frequency combs in the hard X-ray region.

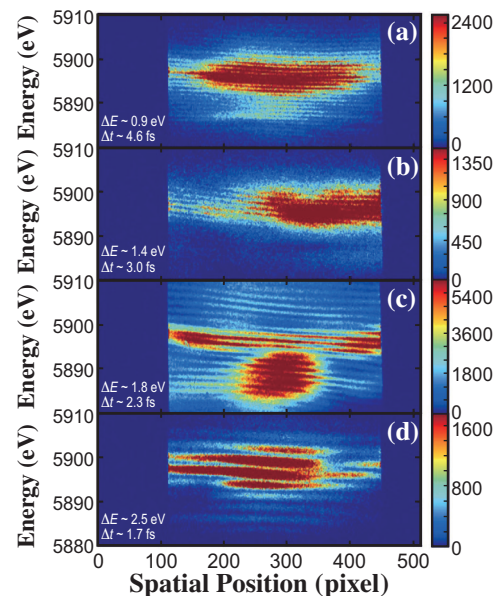


Fig. 3. Selected single-shot ASE spectra of the Mn $K\alpha$ line using MnO_2 films as a gain medium. Spectra with increasing fringe spacings ΔE from ~ 0.9 to 2.5 eV (a–d) are shown, the corresponding time delays Δt between two pulses that cause such interference are also shown in the figure. Each ASE spectrum corresponds to phase-stable femtosecond X-ray pulse pairs with up to $\sim 3 \times 10^7$ photons.

Uwe Bergmann

Dept. of Physics, University of Wisconsin-Madison, USA

Email: ubergmann@wisc.edu

References

- [1] Y. Zhang, T. Kroll, C. Weninger, Y. Michine, F. D. Fuller, D. Zhu, R. Alonso-Mori, D. Sokaras, A. Lutman, A. Halavanau, C. Pellegrini, A. Benediktovitch, M. Yabashi, I. Inoue, Y. Inubushi, T. Osaka, J. Yamada, G. Babu, D. Salpekar, F. N. Sayed, P. M. Ajayan, J. Kern, J. Yano, V. K. Yachandra, H. Yoneda, N. Rohringer, U. Bergmann: *Proc. Natl Acad. Sci.* **119** (2022) e2119616119.
- [2] T. Kroll *et al.*: *Phys. Rev. Lett.* **120** (2018) 133203.
- [3] N. Rohringer *et al.*: *Nature* **481** (2012) 488.
- [4] H. Yoneda *et al.*: *Nature* **524** (2015) 446.
- [5] C. Weninger and N. Rohringer: *Phys. Rev. A* **90** (2014) 063828.